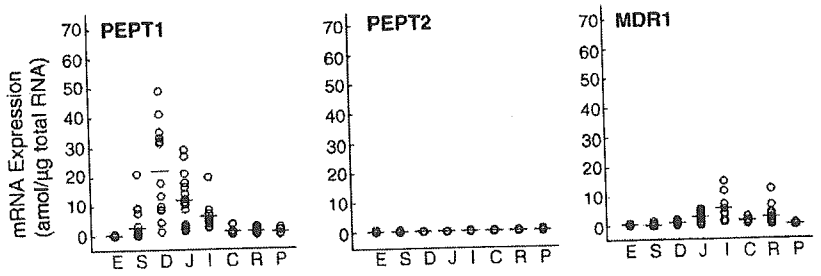

Fig. 1. mRNA expression of PEPT1, PEPT2 and MDR1 along the digestive tract (esophagus (E), stomach (S), duodenum (D), jejunum (J), ileum (I), colon (C), rectum (R)) and pancreas (P). Total cellular RNA was extracted from each tissue sample, and reverse-transcribed. The mRNA levels were determined by real-time PCR using an ABI prism 7700 sequence detector.

duodenum, jejunum, ileum, colon and rectum) and pancreas. As shown in Fig. 1 left, PEPT1 mRNA is highly expressed in the small intestine (duodenum > jejunum > ileum), but is not expressed or only slightly expressed in the esophagus, colon, rectum and pancreas. In the stomach, some patients showed a high level of PEPT1 mRNA. The tissue which showed the highest expression level was the duodenum (22.0 ± 4.23 amol/μg RNA). In contrast to PEPT1 mRNA, PEPT2 mRNA was not expressed in all tissues examined (Fig. 1 middle).

3.2. Western blot analysis

Fig. 2 shows Western blot analyses using crude membranes from each tissue. A primary band of about 80 kDa of PEPT1 protein was detected in the stomach, duodenum, jejunum and ileum, as observed in the mRNA analyses. In other tissues, no PEPT1 protein was detected. In the case of PEPT2 protein, there were no detectable bands in the tissue samples from along the digestive tracts (data not shown). The protein band of Na^+/K^+-ATPase was detected in all specimens (Fig. 2).

3.3. PEPT1 in the stomach

There is no expression of PEPT1 protein in the rat stomach [18]. On the other hand, the present study has demonstrated that some patients had a relatively high level of PEPT1 in the stomach, although there were interindividual differences. To clarify the distribution of PEPT1 in the gastric mucosa, fundus (the upper-third: U), body (the middle-third: M) and antrum (the lower-third: L) mucosa were assessed for PEPT1 protein expression when sections were available from one patient. As shown in Fig. 3,

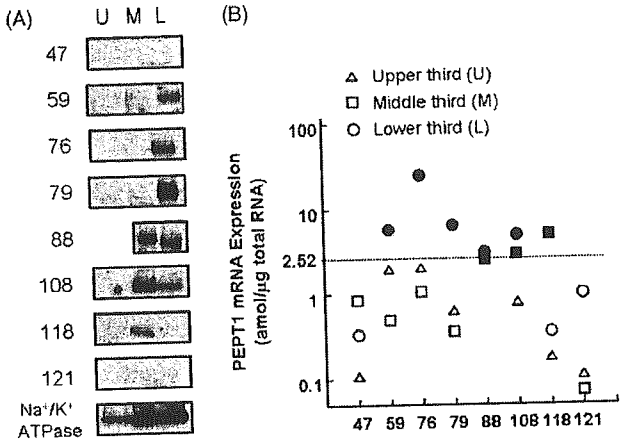

Fig. 3. PEPT1 expression in the gastric mucosa. (A) Crude membranes were isolated from the upper-third (U), middle-third (M) and lower-third (L) of the gastric mucosa from eight patients and subjected to Western blot analyses (50 μg protein/lane) for PEPT1 and Na^+/K^+-ATPase. Conditions for Western blotting were identical to those in Fig. 2. For Na^+/K^+-ATPase, representative data are shown. A sample for the upper-third of patient 88 was not obtained. (B) Relationship between mRNA and protein expression levels of PEPT1 in gastric mucosa. Closed symbols represent the samples with PEPT1 protein expression. When the mRNA level was more than 2.52 amol/μg of total RNA, the band for PEPT1 protein was detected.

PEPT1 protein was expressed in the antral mucosa in most cases, and well correlated with mRNA expression level. When the mRNA level was more than 2.52 amol/μg of total RNA, the band for PEPT1 protein was detected.

These expressional patterns and the histological diagnosis suggested that intestinal metaplasia may induce the expression of PEPT1 in the stomach. Intestinal metaplasia primarily affects the antrum in a patchy fashion, and the superficial gastric epithelium is replaced by intestinal goblet and absorptive cells [19]. Using paraffin sections

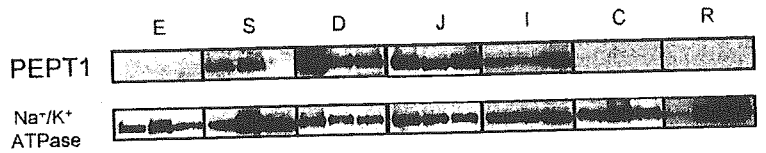

Fig. 2. Western blot analyses of crude membranes isolated from human tissues along the digestive tract for PEPT1 and Na^+/K^+ ATPase. Crude membranes were isolated from each tissue and subjected to Western blotting (50 μg protein/lane). Abbreviations for each tissue are identical to those in Fig. 1. PEPT1 protein was identified using affinity-purified anti-PEPT1 antibody (1:500 dilution). After the membranes were deprobed, Na^+/K^+-ATPase protein was detected by the mouse monoclonal anti Na^+/K^+-ATPase antibody (1:10,000).

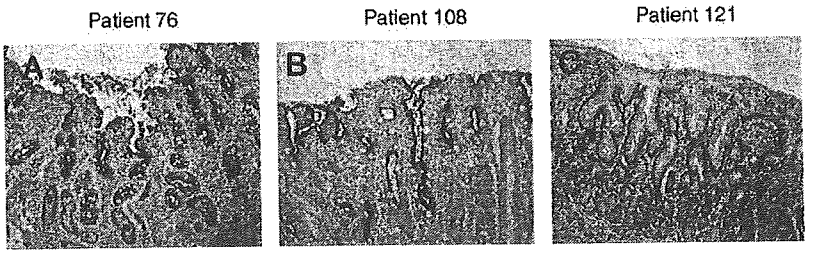

Fig. 4. Localization of CD10 in the intestinal metaplasia. (A and B) CD10 can be seen along the brush-border membranes of the luminal surface of the epithelium in antral mucosa from patients 76 and 108 (original magnification ×50). (C) Hematoxilin–eosin staining of antral mucosa from patient 121.

of antral mucosa from patients 76, 108 and 121, immunostaining for CD10 was carried out. CD10, also known as enkephalinase, has been shown to localize to the brush-border membranes of absorptive small intestinal enterocytes [20]. CD10 was positively expressed along the luminal surface of the epithelium of patients 76 and 108 (Fig. 4A and B), but not patient 121 (data not shown). Hematoxilin–eosin staining revealed that intestinal metaplasia did not occurr in patient 121 (Fig. 4C).

3.4. Comparison of mRNA expression levels of PEPT1 with those of amino acid transporters in the digestive tract

We next examined the expression profile of amino acid transporters in the digestive tract to compare with PEPT1. The human amino acid transporters examined here were mainly neutral amino acid transporters and reported to be important for intestinal epithelial transport, i.e., system B^0 (B^0AT1) [9,10], system ASC (ASCT2) [21], system $b^{0,+}$ ($b^{0,+}AT$) [22], system L (LAT1 [23,24] and LAT2 [25–27]), system y^+L, (y^+LAT1) [28] and system A (ATA2) [29]. It has been demonstrated that B^0AT1, ASCT2 and $b^{0,+}AT$ localized at the brush-border membranes of epithelial cells, whereas LAT1, LAT2, y^+LAT1 and ATA2 localized at the basolateral membranes.

Fig. 5 shows the mRNA expression levels along the digestive tract for the amino acid transporters localized to brush-border membranes: B^0AT1, ASCT2 and $b^{0,+}AT$. These three transporters exhibited distinguishable expression patterns. B^0AT1 mRNA levels were increased from duodenum to ileum like MDR1 mRNA levels. ASCT2 showed little expression in the small intestine, but significant expression in the large intestine (colon and rectum). In contrast, $b^{0,+}AT$ exhibited little expression in the digestive tract except for the stomach.

Fig. 6 shows the mRNA expression levels along the digestive tract for the amino acid transporters localized to basolateral membranes: LAT1, LAT2, y^+LAT1 and ATA2. ATA2 showed a strong expression in the tissues tested. LAT1 was preferentially expressed in the esophagus, stomach and pancreas, as compared with the small and large intestine. The expression of LAT2 was abundant in the stomach and rectum, and modest in the small intestine

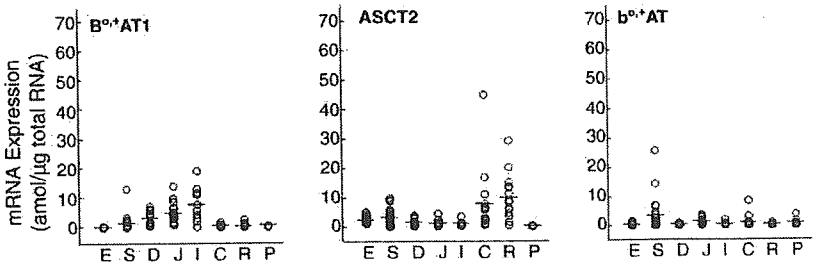

Fig. 5. mRNA expression of brush-border membrane-localized amino acid transporters B^0AT1, ASCT2 and $b^{0,+}AT$ along the digestive tract and pancreas. Abbreviations for each tissue and experimental methods are identical to those in Fig. 1.

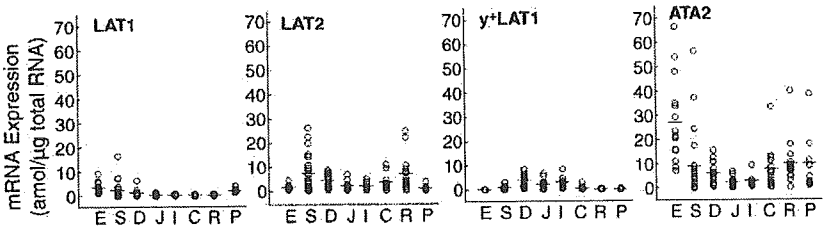

Fig. 6. mRNA expression of basolateral membrane-localized amino acid transporters LAT1, LAT2, y^+LAT1 and ATA2 along the digestive tract and pancreas. Abbreviations for each tissue and experimental methods are identical to those in Fig. 1.

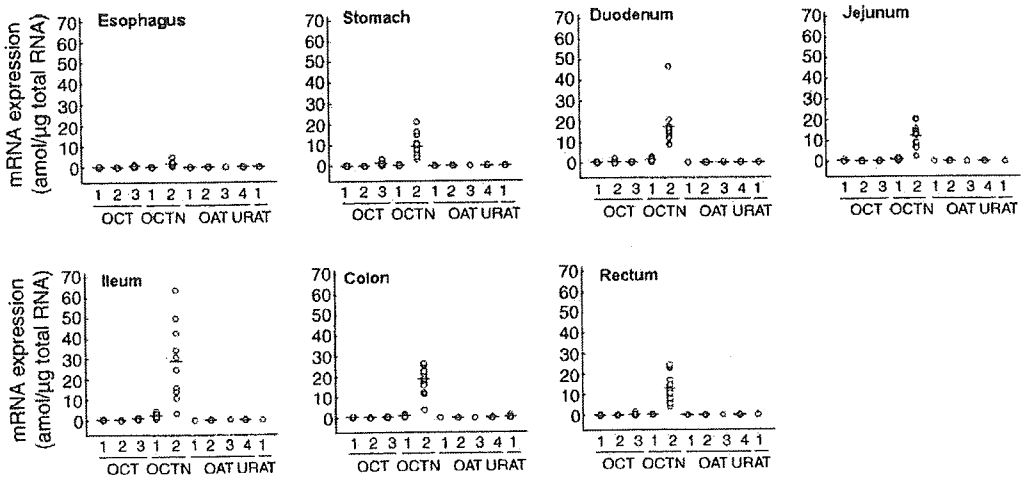

Fig. 7. mRNA expression of organic ion transporters along the digestive tract. Tested transporters are as follows: OCT1–3, OCTN1 and 2, OAT1–4 and URAT1. Experimental methods are identical to those in Fig. 1.

(duodenum, jejunum and ileum). In contrast, y^+LAT1 was predominantly expressed in the small intestine (duodenum, jejunum and ileum) with little expression in other tissues.

PEPT1 also works as a drug transporter. To compare the mRNA expression level of PEPT1 with other drug transporters, we selected organic ion transporter family including organic cation transporters (OCT1–3), organic cation/carnitine transporters (OCTN1 and 2), organic anion transporters (OAT1–4) and urate transporter (URAT1). These transporters are mainly expressed in the kidney [11] and play important roles for renal secretion of ionic drugs [30], but some transporters were suggested to mediate the intestinal secretion of drugs [31]. As shown in Fig. 7, there was little expression for organic ion transporters except for OCTN2. OCTN2 exhibited a similar expression level of PEPT1 in the intestine. In addition to intestine, OCTN2 exhibited abundant expression in the stomach, colon and rectum.

4. Discussion

In the present study, we have demonstrated that the mRNA expression level of PEPT1 is higher in the duodenum and jejunum than that of B^0AT1, ASCT2 and $b^{0,+}$AT, which are localized at the brush-border membranes, and is equal to that of B^0AT1 in the ileum. Previous works showed that luminal contents after protein ingestion mostly consist of two to six amino acids [32], and that most of the dipeptidase activity is located in the cytoplasm of mucosal cells [33]. Thus, higher expression levels of PEPT1 than amino acid transporters at brush-border membranes should support the nutritional importance of the intestinal absorption of small peptides for protein nutrition. The high expression levels of intestinal PEPT1 also emphasize the pharmacological implication of peptide transporters. The peptide-like drugs transported by PEPT1 showed good oral bioavailability [3]. Transport abilities of PEPT1, with great flexibility for structural modification, and high expression of PEPT1 in the small intestine should be helpful for drug development to improve the intestinal absorption of poorly absorbed drugs.

The expression level of PEPT1 mRNA showed a peak in the duodenum, and gradually decreased to the ileum. Interestingly, the expression gradient of B^0AT1 mRNA is completely inversed to that of PEPT1. These reciprocal axial gradients in the mRNA expression of PEPT1 and B^0AT1 well correspond to the transport activities of small peptides [34,35] and amino acids for system B [36], and may have physiological relevance and importance to the maintenance of optimal protein nutrition [37]. Namely, the ingested proteins are digested by the membrane-bound peptidases to generate a major portion of the absorbable products, namely, amino acids and small peptides. Though these peptidases are present throughout the small intestine, levels of activity are much higher in the ileum than in the jejunum [38], indicating that the concentrations of free amino acids in the lumen are gradually increased, while the luminal concentration of small peptides are gradually decreased as the luminal contents move along the intestine. Furthermore, K_m values of typical substrates for PEPT1 (glycylsarcosine) [39] and B^0AT1 (leucine) [10] were about 1 mM, suggesting that both transporters have similar kinetic parameters. It is, therefore, suggested that the efficient absorption of digestive products of proteins may be achieved by a good correlation between the expression profiles for PEPT1 and B^0AT1 and the luminal concentrations of the corresponding substrates along the intestine.

Using tissue biopsy samples, Gutmann et al. [40] demonstrated that the mRNA expression of human breast cancer resistance protein (BCRP) was maximal in the duodenum and decreased continuously down to the rectum [40]. This expression profile is contrast to that of MDR1 mRNA expression (Fig. 1 right), suggesting that BCRP and

MDR1 also complement the transport function each other along the digestive tract as the substrate specificity of both transporters is partially overlapping [41]. Taken together, reciprocal expression of functionally related membrane transporters along the digestive tract should be responsible for the efficient biological systems in physiology and pharmacology.

Recently, Dave et al. [42] examined the expression of heteromeric amino acid transporters along the murine intestine. Their major findings related to our study were as follows: (i) the main sites of mRNA expression of absorptive amino acid transporters ($b^{0,+}$AT, LAT2 and y^+LAT1) were the jejunum and ileum; (ii) a substantial level of LAT2 mRNA was found in the stomach, an organ not previously recognized as a major site of amino acid absorption and (iii) LAT1 was most abundant in brain and weakly expressed in the intestine except for the stomach. Most of these findings were also confirmed in the human intestine, although the expression levels of $b^{0,+}$AT, LAT2 and y^+LAT1were not so high in the human intestine as compared to mouse intestine. Mutations in $b^{0,+}$AT lead to the hereditary disease cystinuria [22], and characterized by renal loss and altered intestinal absorption of cationic amino acids and cystine. Interestingly, patients with cystinuria do not exhibit obvious symptoms of protein malabsorption because the affected amino acids are absorbed adequately in the form of small peptides [43]. The much higher levels of PEPT1 than $b^{0,+}$AT explain this compensation.

In the present study, PEPT1 was found to be expressed in the stomach, induced by intestinal metaplasia. Intestinal metaplasia is characterized by the transdifferentiation of gastric epithelial cells to an intestinal phenotype [19]. Several intestinal-specific gene products such as trefoil peptides [44] were reported to be expressed in the stomach after intestinal metaplasia. *CDX2*, an intestine-specific transcription factor belonging to the *caudal*-related homeobox gene family, was involved in the induction of intestinal metaplasia of the stomach [45]. We have recently clarified the significant role of Sp1 in the basal transcriptional regulation of PEPT1 [46], but the mechanisms of intestine-specific expression of PEPT1 have not been clarified yet. CDX2 may also be responsible for the small intestinal and gastric expression of PEPT1.

Among organic ion transporters tested, only OCTN2 showed significant expression in the intestine, as the same expression level of PEPT1. The physiological substrate for OCTN2 is the carnitine, and mutations in this protein cause the autosomal recessive systemic carnitine deficiency [47]. In addition to carnitine, OCTN2 can transport various drugs such as verapamil [48]. This transport activity and abundant expression in the intestine suggested the pharamcokinetic role of OCTN2 for intestinal absorption like PEPT1. Using *Oct1* knockout mice, it was demonstrated that Oct1 plays important roles for intestinal excretion of cationic drugs [49]. But, the present expression analyses revealed that there was little expression of OCT1 along the digestive tract. Further studies are needed to clarify the clinical implication of intestinal OCT1.

In conclusion, we demonstrated the expression profile of PEPT1, amino acid transporters and organic ion transporters along the human digestive tract. The reciprocal distribution of PEPT1 and B^0AT1 may contribute to the efficient absorption of digestive products of ingested proteins. PEPT1 expression in the stomach is caused by intestinal metaplasia. OCTN2 is also abundantly expressed in the intestine. These findings may provide useful information about enteral nutrition, gastric pathology and pharmacology.

Acknowledgements

This work was supported by the 21st Century COE Program "Knowledge Information Infrastructure for Genome Science", a Grant-in-Aid for Research on Advanced Medical Technology from the Ministry of Health, Labor and Welfare of Japan, and a grant from the Astellas Foundation for Research on Metabolic Disorders.

References

[1] Adibi SA. The oligopeptide transporter (Pept-1) in human intestine: biology and function. Gastroenterology 1997;113:332–40.
[2] Daniel H. Molecular and integrative physiology of intestinal peptide transport. Annu Rev Physiol 2004;66:361–84.
[3] Terada T, Inui K. Peptide transporters: structure, function, regulation and application for drug delivery. Curr Drug Metab 2004;5:85–94.
[4] Christensen HN. Role of amino acid transport and countertransport in nutrition and metabolism. Physiol Rev 1990;70:43–77.
[5] Verrey F, Closs EI, Wagner CA, Palacin M, Endou H, Kanai Y. CATs and HATs: the SLC7 family of amino acid transporters. Pflugers Arch 2004;447:532–42.
[6] Verrey F, Ristic Z, Romeo E, Ramadam T, Makrides V, Dave MH, et al. Novel renal amino acid transporters. Annu Rev Physiol 2005;67:557–72.
[7] Stevens BR, Ross HJ, Wright EM. Multiple transport pathways for neutral amino acids in rabbit jejunal brush border vesicles. J Membr Biol 1982;66:213–25.
[8] Munck BG, Munck LK. Phenylalanine transport in rabbit small intestine. J Physiol 1994;480:99–107.
[9] Seow HF, Broer S, Broer A, Bailey CG, Potter SJ, Cavanaugh JA, et al. Hartnup disorder is caused by mutations in the gene encoding the neutral amino acid transporter SLC6A19. Nat Genet 2004;36:999–1002.
[10] Kleta R, Romeo E, Ristic Z, Ohura T, Stuart C, Arcos-Burgos M, et al. Mutations in SLC6A19, encoding B^0AT1, cause Hartnup disorder. Nat Genet 2004;36:1003–7.
[11] Motohashi H, Sakurai Y, Saito H, Masuda S, Urakami Y, Goto M, et al. Gene expression levels and immunolocalization of organic ion transporters in the human kidney. J Am Soc Nephrol 2002;13:866–74.
[12] Masuda S, Uemoto S, Goto M, Fujimoto Y, Tanaka K, Inui K. Tacrolimus therapy according to mucosal MDR1 levels in small-bowel transplant recipients. Clin Pharmacol Ther 2004;75:352–61.
[13] Ashida K, Katsura T, Motohashi H, Saito H, Inui K. Thyroid hormone regulates the activity and expression of the peptide transporter PEPT1 in Caco-2 cells. Am J Physiol Gastrointest Liver Physiol 2002;282:G617–23.

[14] Hashida T, Masuda S, Uemoto S, Saito H, Tanaka K, Inui K. Pharmacokinetic and prognostic significance of intestinal MDR1 expression in recipients of living-donor liver transplantation. Clin Pharmacol Ther 2001;69:308–16.
[15] Zimmermann C, Gutmann H, Hruz P, Gutzwiller JP, Beglinger C, Drewe J. Mapping of MDR1 and MRP1–5 mRNA expression along the human intestinal tract. Drug Metab Dispos 2005;33: 219–24.
[16] Mouly S, Paine MF. P-glycoprotein increases from proximal to distal regions of human small intestine. Pharm Res 2003;20:1595–9.
[17] Fojo AT, Ueda K, Slamon DJ, Poplack DG, Gottesman MM, Pastan I. Expression of a multidrug-resistance gene in human tumors and tissues. Proc Natl Acad Sci USA 1987;84:265–9.
[18] Ogihara H, Saito H, Shin BC, Terada T, Takenoshita S, Nagamachi Y, et al. Immuno-localization of H^+/peptide cotransporter in rat digestive tract. Biochem Biophys Res Commun 1996;220:848–52.
[19] Fenoglio-Preiser CM, Lantz PE, Listrom MB, Davis M, Rilke FO. Metaplasia. Gastrointestinal pathology: an atlas and text. New York: Raven, 1989. p. 154–7.
[20] Trejdosiewicz LK, Malizia G, Oakes J, Losowsky MS, Janossy G. Expression of the common acute lymphoblastic leukaemia antigen (CALLA gp100) in the brush border of normal jejunum and jejunum of patients with coeliac disease. J Clin Pathol 1985;38:1002–6.
[21] Kekuda R, Prasad PD, Fei YJ, Torres-Zamorano V, Sinha S, Yang-Feng TL, et al. Cloning of the sodium-dependent, broad-scope, neutral amino acid transporter B^0 from a human placental choriocarcinoma cell line. J Biol Chem 1996;271:18657–61.
[22] Feliubadalo L, Font M, Purroy J, Rousaud F, Estivill X, Nunes V, et al. Non-type I cystinuria caused by mutations in SLC7A9, encoding a subunit ($b^{0,+}$AT) of rBAT, International Cystinuria Consortium. Nat Genet 1999;23:52–7.
[23] Kanai Y, Segawa H, Miyamoto K, Uchino H, Takeda E, Endou H. Expression cloning and characterization of a transporter for large neutral amino acids activated by the heavy chain of 4F2 antigen (CD98). J Biol Chem 1998;273:23629–32.
[24] Mastroberardino L, Spindler B, Pfeiffer R, Skelly PJ, Loffing J, Shoemaker CB, et al. Amino-acid transport by heterodimers of 4F2hc/CD98 and members of a permease family. Nature 1998;395: 288–91.
[25] Pineda M, Fernandez E, Torrents D, Estevez R, Lopez C, Camps M, et al. Identification of a membrane protein, LAT-2, that co-expresses with 4F2 heavy chain, an L-type amino acid transport activity with broad specificity for small and large zwitterionic amino acids. J Biol Chem 1999;274:19738–44.
[26] Segawa H, Fukasawa Y, Miyamoto K, Takeda E, Endou H, Kanai Y. Identification and functional characterization of a Na^+-independent neutral amino acid transporter with broad substrate selectivity. J Biol Chem 1999;274:19745–51.
[27] Rossier G, Meier C, Bauch C, Summa V, Sordat B, Verrey F, et al. LAT2, a new basolateral 4F2hc/CD98-associated amino acid transporter of kidney and intestine. J Biol Chem 1999;274: 34948–54.
[28] Torrents D, Mykkanen J, Pineda M, Feliubadalo L, Estevez R, de Cid R, et al. Identification of SLC7A7, encoding y^+LAT-1, as the lysinuric protein intolerance gene. Nat Genet 1999;21:293–6.
[29] Sugawara M, Nakanishi T, Fei YJ, Huang W, Ganapathy ME, Leibach FH, et al. Cloning of an amino acid transporter with functional characteristics and tissue expression pattern identical to that of system A. J Biol Chem 2000;275:16473–7.
[30] Inui K, Masuda S, Saito H. Cellular and molecular aspects of drug transport in the kidney. Kidney Int 2000;58:944–58.
[31] Jonker JW, Schinkel AH. Pharmacological and physiological functions of the polyspecific organic cation transporters: OCT1, 2 and 3 (SLC22A1–3). J Pharmacol Exp Ther 2004;308:2–9.
[32] Adibi SA, Mercer DW. Protein digestion in human intestine as reflected in luminal, mucosal, and plasma amino acid concentrations after meals. J Clin Invest 1973;52:1586–94.
[33] Kim YS, Birtwhistle W, Kim YW. Peptide hydrolases in the bruch border and soluble fractions of small intestinal mucosa of rat and man. J Clin Invest 1972;51:1419–30.
[34] Crampton RF, Lis MT, Matthews DM. Sites of maximal absorption and hydrolysis of two dipeptides by rat small intestine in vivo. Clin Sci 1973;44:583–94.
[35] Schedl HP, Burston D, Taylor E, Matthews DM. Kinetics of mucosal influx of glycylsarcosine, glycine and leucine into hamster jejunum and ileum in vitro. Clin Sci (Lond) 1979;56:25–31.
[36] Munck LK, Munck BG. Variation in amino acid transport along the rabbit small intestine. Mutual jejunal carriers of leucine and lysine. Biochim Biophys Acta 1992;1116:83–90.
[37] Ganapathy V, Brandsch M, Leibach FH. Intestinal transport of amino acids and proteins. In: Johnson LR, editor. Physiology of the gastrointestinal tract. 3rd ed., New York: Raven; 1994. p. 1773–94.
[38] Das M, Radhakrishnan AN. A comparative study of the distribution of soluble and particulate glycyl-L-leucine hydrolase in the small intestine. Clin Sci Mol Med 1974;46:501–10.
[39] Terada T, Sawada K, Saito H, Hashimoto Y, Inui K. Functional characteristics of basolateral peptide transporter in the human intestinal cell line Caco-2. Am J Physiol 1999;276:G1435–41.
[40] Gutmann H, Hruz P, Zimmermann C, Beglinger C, Drewe J. Distribution of breast cancer resistance protein (BCRP/ABCG2) mRNA expression along the human GI tract. Biochem Pharmacol 2005;70:695–9.
[41] Litman T, Brangi M, Hudson E, Fetsch P, Abati A, Ross DD, et al. The multidrug-resistant phenotype associated with overexpression of the new ABC half-transporter, MXR (ABCG2). J Cell Sci 2000;113:2011–21.
[42] Dave MH, Schulz N, Zecevic M, Wagner CA, Verrey F. Expression of heteromeric amino acid transporters along the murine intestine. J Physiol 2004;558:597–610.
[43] Hellier MD, Holdsworth CD, Perrett D, Thirumalai C. Intestinal depeptide transport in normal and cystinuric subjects. Clin Sci 1972;43:659–68.
[44] Leung WK, Yu J, Chan FK, To KF, Chan MW, Ebert MP, et al. Expression of trefoil peptides (TFF1, TFF2, and TFF3) in gastric carcinomas, intestinal metaplasia, and non-neoplastic gastric tissues. J Pathol 2002;197:582–8.
[45] Yuasa Y. Control of gut differentiation and intestinal-type gastric carcinogenesis. Nat Rev Cancer 2003;3:592–600.
[46] Shimakura J, Terada T, Katsura T, Inui K. Characterization of the human peptide transporter PEPT1 promoter: Sp1 functions as a basal transcriptional regulator of human PEPT1. Am J Physiol Gastrointest Liver Physiol 2005;289:G471–7.
[47] Nezu J, Tamai I, Oku A, Ohashi R, Yabuuchi H, Hashimoto N, et al. Primary systemic carnitine deficiency is caused by mutations in a gene encoding sodium ion-dependent carnitine transporter. Nat Genet 1999; 21:91–4.
[48] Ohashi R, Tamai I, Yabuuchi H, Nezu J, Oku A, Sai Y, et al. Na^+-dependent carnitine transport by organic cation transporter (OCTN2): its pharmacological and toxicological relevance. J Pharmacol Exp Ther 1999;291:778–84.
[49] Jonker JW, Wagenaar E, Mol CA, Buitelaar M, Koepsell H, Smit JW, et al. Reduced hepatic uptake and intestinal excretion of organic cations in mice with a targeted disruption of the organic cation transporter 1 (Oct1 [Slc22a1]) gene. Mol Cell Biol 2001;21:5471–7.

Available online at www.sciencedirect.com
SCIENCE DIRECT®
Biochemical and Biophysical Research Communications 338 (2005) 1788–1790
BBRC
www.elsevier.com/locate/ybbrc

GPR40 gene expression in human pancreas and insulinoma

Tsutomu Tomita [a], Hiroaki Masuzaki [a,*], Michio Noguchi [a], Hiroshi Iwakura [a], Junji Fujikura [a], Tomohiro Tanaka [a], Ken Ebihara [a], Junichiro Kawamura [b], Izumi Komoto [b], Yoshiya Kawaguchi [b], Koji Fujimoto [b], Ryuichiro Doi [b], Yutaka Shimada [b], Kiminori Hosoda [a], Masayuki Imamura [b], Kazuwa Nakao [a]

[a] *Department of Medicine and Clinical Science, Kyoto University Graduate School of Medicine, Kyoto, Japan*
[b] *Department of Surgery and Surgical Basic Science, Kyoto University Graduate School of Medicine, Kyoto, Japan*

Received 17 October 2005
Available online 2 November 2005

Abstract

To assess gene expression of a membrane-bound G-protein-coupled fatty acid receptor, GPR40, in the human pancreas and islet cell tumors obtained at surgery were analyzed. The mRNA level of the GPR40 gene in isolated pancreatic islets was approximately 20-fold higher than that in the pancreas, and the level was comparable to or rather higher than that of the sulfonylurea receptor 1 gene, which is known to be expressed abundantly in human pancreatic β cells. A large amount of GPR40 mRNA was detected in tissue extracts from two cases of insulinoma, whereas the expression was undetectable in glucagonoma or gastrinoma. The present study demonstrates that GPR40 mRNA is expressed predominantly in pancreatic islets in humans and that GPR40 mRNA is expressed solely in human insulinoma among islet cell tumors. These results indicate that GPR40 is probably expressed in pancreatic β cells in the human pancreas.

Keywords: G-protein-coupled receptor; GPR40; Islet of Langerhans; Pancreatic β cell; Insulinoma; Fatty acid; Insulin secretion

Fatty acids (FAs), especially long chain FAs, augment glucose-stimulated insulin secretion (GSIS) from the pancreas [1]. To date, however, the entire mechanism whereby FAs acutely induce GSIS augmentation has not been fully elucidated [2]. In addition, chronic FA exposure causes marked deterioration of β cell function, which is referred to as lipotoxicity [3,4].

GPR40, a membrane-bound G-protein-coupled receptor, is reported to be preferentially expressed in pancreatic β cells in rodents and is involved in the regulation of GSIS after acute exposure to mid- or long-chain FAs in in vitro experiments [5]. A recent study regarding GPR40 knockout mice and β cell-specific GPR40 transgenic mice suggests the possible involvement of GPR40 in diabetes mellitus [6]. Although these findings suggest the implication of GPR40 in the regulation of insulin secretion and glucose homeostasis, gene expression of GPR40 in humans has not been fully elucidated [2,7]. The present study was designed to investigate GPR40 mRNA expression in the pancreas and islet cell tumors in humans.

Materials and methods

Participants, tissue sampling, and pancreatic islet isolation. The present study was performed according to the Declaration of Helsinki and approved by the Ethical Committee on Human Research of Kyoto University Graduate School of Medicine (No. 508, 2003). Signed informed consent was obtained from all patients in the present study. Normal pancreata were obtained from four patients with pancreatic cancer and one patient with insulinoma at the time of surgery. Sample margins contained no signs of tumor invasion, thus these pancreatic samples were thought to be free of tumor. In addition, insulinoma ($n = 2$), glucagonoma ($n = 1$), and gastrinoma ($n = 1$) were collected at surgery. Pancreatic islet tissues were promptly isolated from the pancreas through the mince method [8]. After dithizone staining, pancreatic islets were manually collected using a stereomicroscope (SZ-STB1; Olympus, Tokyo, Japan).

* Corresponding author. Fax: +81 75 771 9452.
E-mail address: hiroaki@kuhp.kyoto-u.ac.jp (H. Masuzaki).

0006-291X/$ - see front matter © 2005 Elsevier Inc. All rights reserved.
doi:10.1016/j.bbrc.2005.10.161

Table 1
Sequences of TaqMan primers and probes

Gene	GenBank Accession No.	Probe (FAM-5′ → 3′-TAMRA)	Primers[a] (5′ → 3′)
GPR40	NM005303	TCTGCCCTTGGCCATCACAGCCT	*f* GCCCGCTTCAGCCTCTCT
			r GAGGCAGCCCACGTAGCA
SUR1	NM000352	CCTCACCAACTACCAACGGCTCTGCG	*f* GCTGCCCATCGTTATGAGGG
			r GAATGTCCTTCCGCACCTGG
GAPDH	NM002046	CCTCAAGGGCATCCTGGGCTACACTG	*f* TGAAGCAGGCGTCGGAGG
			r GCTGTTGAAGTCAGAGGAGACC

Abbreviations: FAM, 6-carboxyfluorescein; TAMRA, 6-carboxytetramethylrhodamine.
[a] Forward primers are designated by *f* and reverse primers by *r*.

Quantification of mRNA expression of GPR40 and SUR1. We measured mRNA expression of genes encoding GPR40 and sulfonylurea receptor 1 (SUR1) [9]. Total RNA was extracted using the QIAGEN RNeasy Mini Kit (QIAGEN GmbH, Hilden, Germany) [10] and treated with DNase I to avoid contamination of genomic DNA, because GPR40 gene is a single exon one. First strand cDNA was synthesized by random hexamer primed reverse transcription using SuperScript II reverse transcriptase (Invitrogen, Carlsbad, CA) [11]. The mRNA level was quantified by the TaqMan PCR method using an ABI PRISM 7700 Sequence Detector (Applied Biosystems, Foster City, CA) as described [12]. RT-minus samples served as a control to exclude the amplification of potential genomic DNA contamination. To calculate the copy number of each mRNA, standard curves were generated using synthesized oligo DNA fragments (Proligo Japan, Kyoto, Japan) containing the PCR amplicon region. The mRNA level of each gene was normalized to that of GAPDH and expressed in arbitrary units as relative to the GPR40 mRNA level in the normal pancreas from case 1. Table 1 summarizes the sequences of primers and probes used in the present study.

Results

Expression of GPR40 mRNA in human pancreas and isolated pancreatic islets

By use of total RNA samples from patients who underwent pancreatectomy, GPR40 mRNA expression in the human pancreas was examined. GPR40 mRNA was detected in normal pancreata obtained from four patients with pancreatic cancer and one patient with insulinoma, where the relative expression values were from 0.70 to 2.08 in arbitrary unit (1.16 ± 0.39, means $\pm$ SEM). The GPR40 mRNA level in freshly prepared isolated pancreatic islets was approximately 20-fold higher than that in the pancreas from the same individuals (Fig. 1).

To evaluate the expression of GPR40 in human pancreatic islets, we measured gene expression of sulfonylurea receptor, which is known to be expressed abundantly in pancreatic β cells. The estimated mRNA copy number of the GPR40 gene in isolated pancreatic islets was comparable to or rather higher than that of the sulfonylurea receptor 1 (SUR1) gene (Fig. 1).

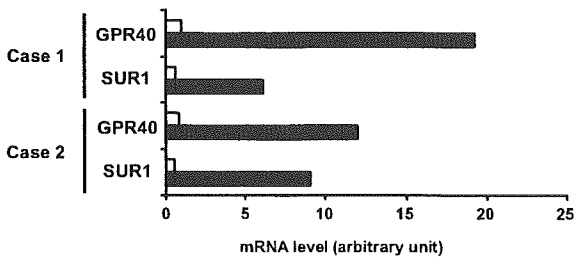

Fig. 1. GPR40 and SUR1 mRNA expression in human pancreas and pancreatic islet. Total RNA extracted from human pancreata (open bars) and pancreatic islets (closed bars) was analyzed in two patients. The mRNA level for each gene was normalized to that of GAPDH.

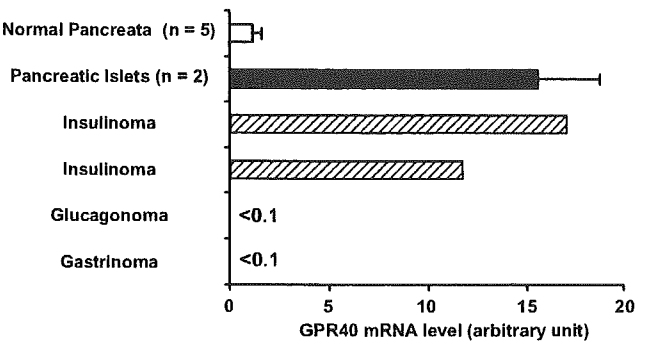

Fig. 2. GPR40 mRNA expression in human pancreas, pancreatic islet, and islet cell tumors. Total RNA extracted from the normal human pancreas (the open bar, $n = 5$), pancreatic islets (the closed bar, $n = 2$), and islet cell tumors (hatched bars). The GPR40 mRNA level was normalized to that of GAPDH. Data are expressed as means $\pm$ SEM in the pancreas and pancreatic islets.

A large amount of GPR40 mRNA expression in insulinoma tissues

We next explored the expression of GPR40 mRNA in islet cell tumors including insulinoma, glucagonoma, and gastrinoma. GPR40 mRNA was detected in tissue extracts from two cases of insulinoma, which was comparable to that in human pancreatic islets (Fig. 2). In contrast, GPR40 mRNA was undetectable in tissue extracts from glucagonoma or gastrinoma (Fig. 2).

Discussion

As pancreatic tissues are extremely vulnerable to postmortem autolysis, freshly prepared specimens obtained at operation have a great advantage for the precise analysis of the GPR40 mRNA level. Using expeditiously isolated pancreatic islets from the pancreatic tissue obtained during surgery, the present study demonstrates that a large amount of GPR40 mRNA is expressed in pancreatic islets in humans. Levels of GPR40 mRNA expression in

pancreatic islets are 20-fold higher than those of the whole pancreas in the same individuals. The present study also demonstrates that a large amount of GPR40 mRNA is expressed in the insulinoma tissue. In contrast, the mRNA was not detected in glucagonoma or gastrinoma. This is the first demonstration of GPR40 mRNA expression in human insulinoma. These findings indicate that GPR40 is probably expressed mainly in β cells in the human pancreas.

It is important to note that the mRNA level of GPR40 is comparable to that of SUR1 in human pancreatic islets, which is abundantly expressed in human pancreatic β cells and works as a target of anti-diabetic sulfonylurea agents [13]. Thus, the present study indicates that GPR40 is expressed in β cells in the human pancreas, suggesting its involvement in the regulation of insulin secretion.

Acknowledgments

We are grateful to Ms. M. Nagamoto for her excellent technical assistance. This study was supported in part by a research grant from Special Coordination Funds for Promoting Science and Technology (JST, Japan), a Grant-in-Aid for Scientific Research (S2) (16109007), a Grant-in-Aid for Scientific Research (B2) (16390267), a Grant-in-Aid for Exploratory Research (16659243), a Grant-in-Aid for Scientific Research on Priority Areas (15081101) (The Japanese Ministry of Education, Culture, Sports, Science and Technology), a Grant-in-Aid for Research (The Japanese Ministry of Health, Labor and Welfare), and a research award from the Japan Foundation for Applied Enzymology, the Yamaguchi Endocrine Research Association, The Cell Science Research Foundation, the Takeda Medical Research Foundation, the Smoking Research Foundation, and the Metabolic Syndrome Research Foundation.

References

[1] D.T. Stein, B.E. Stevenson, M.W. Chester, M. Basit, M.B. Daniels, S.D. Turley, J.D. McGarry, The insulinotropic potency of fatty acids is influenced profoundly by their chain length and degree of saturation, J. Clin. Invest. 100 (1997) 398–403.

[2] C.P. Briscoe, M. Tadayyon, J.L. Andrews, W.G. Benson, J.K. Chambers, M.M. Eilert, C. Ellis, N.A. Elshourbagy, A.S. Goetz, D.T. Minnick, P.R. Murdock, H.R. Sauls Jr., U. Shabon, L.D. Spinage, J.C. Strum, P.G. Szekeres, K.B. Tan, J.M. Way, D.M. Ignar, S. Wilson, A.I. Muir, The orphan G protein-coupled receptor GPR40 is activated by medium and long chain fatty acids, J. Biol. Chem. 278 (2003) 11303–11311.

[3] J.D. McGarry, R.L. Dobbins, Fatty acids, lipotoxicity and insulin secretion, Diabetologia 42 (1999) 128–138.

[4] R.H. Unger, Minireview: weapons of lean body mass destruction: the role of ectopic lipids in the metabolic syndrome, Endocrinology 144 (2003) 5159–5165.

[5] Y. Itoh, Y. Kawamata, M. Harada, M. Kobayashi, R. Fujii, S. Fukusumi, K. Ogi, M. Hosoya, Y. Tanaka, H. Uejima, H. Tanaka, M. Maruyama, R. Satoh, S. Okubo, H. Kizawa, H. Komatsu, F. Matsumura, Y. Noguchi, T. Shinohara, S. Hinuma, Y. Fujisawa, M. Fujino, Free fatty acids regulate insulin secretion from pancreatic beta cells through GPR40, Nature 422 (2003) 173–176.

[6] P. Steneberg, N. Rubins, R. Bartoov-Shifman, M.D. Walker, H. Edlund, The FFA receptor GPR40 links hyperinsulinemia, hepatic steatosis, and impaired glucose homeostasis in mouse, Cell Metab. 1 (2005) 245–258.

[7] K. Kotarsky, N.E. Nilsson, E. Flodgren, C. Owman, B. Olde, A human cell surface receptor activated by free fatty acids and thiazolidinedione drugs, Biochem. Biophys. Res. Commun. 301 (2003) 406–410.

[8] J.L. Cameron, D.G. Mehigan, D.P. Harrington, G.D. Zuidema, Metabolic studies following intrahepatic autotransplantation of pancreatic islet grafts, Surgery 87 (1980) 397–400.

[9] G. Giannaccini, R. Lupi, M.L. Trincavelli, R. Navalesi, L. Betti, P. Marchetti, A. Lucacchini, S. Del Guerra, C. Martini, Characterization of sulfonylurea receptors in isolated human pancreatic islets, J. Cell. Biochem. 71 (1998) 182–188.

[10] H. Iwakura, K. Hosoda, C. Son, J. Fujikura, T. Tomita, M. Noguchi, H. Ariyasu, K. Takaya, H. Masuzaki, Y. Ogawa, T. Hayashi, G. Inoue, T. Akamizu, H. Hosoda, M. Kojima, H. Itoh, S. Toyokuni, K. Kangawa, K. Nakao, Analysis of rat insulin II promoter-ghrelin transgenic mice and rat glucagon promoter-ghrelin transgenic mice, J. Biol. Chem. 280 (2005) 15247–15256.

[11] H. Iwakura, K. Hosoda, R. Doi, I. Komoto, H. Nishimura, C. Son, J. Fujikura, T. Tomita, K. Takaya, Y. Ogawa, T. Hayashi, G. Inoue, T. Akamizu, H. Hosoda, M. Kojima, K. Kangawa, M. Imamura, K. Nakao, Ghrelin expression in islet cell tumors: augmented expression of ghrelin in a case of glucagonoma with multiple endocrine neoplasm type I, J. Clin. Endocrinol. Metab. 87 (2002) 4885–4888.

[12] Y. Li, I. Kishimoto, Y. Saito, M. Harada, K. Kuwahara, T. Izumi, I. Hamanaka, N. Takahashi, R. Kawakami, K. Tanimoto, Y. Nakagawa, M. Nakanishi, Y. Adachi, D.L. Garbers, A. Fukamizu, K. Nakao, Androgen contributes to gender-related cardiac hypertrophy and fibrosis in mice lacking the gene encoding guanylyl cyclase-A, Endocrinology 145 (2004) 951–958.

[13] F.M. Gribble, F. Reimann, Sulphonylurea action revisited: the post-cloning era, Diabetologia 46 (2003) 875–891.

261

Original Paper

Pancreatology

Pancreatology 2006;6:109–116
DOI: 10.1159/000090030

Received: March 29, 2005
Accepted after revision: June 6, 2005
Published online: December 1, 2005

Chemoradiotherapy in Patients with Pancreatic Carcinoma: Phase-I Study with a Fixed Radiation Dose and Escalating Doses of Weekly Gemcitabine

Natsuo Oya[a,b] Keiko Shibuya[a] Takashi Sakamoto[a,b] Takashi Mizowaki[a] Ryuichiro Doi[c] Koji Fujimoto[c] Masayuki Imamura[c] Yasushi Nagata[a] Masahiro Hiraoka[a]

[a]Department of Therapeutic Radiology and Oncology, Graduate School of Medicine, Kyoto University, Kyoto, [b]Department of Radiation Oncology, Graduate School of Medical Sciences, Kumamoto University, Kumamoto, and [c]Department of Surgery and Surgical Basic Sciences, Graduate School of Medicine, Kyoto University, Kyoto, Japan

Key Words
Pancreatic cancer · Chemoradiotherapy · Gemcitabine, maximum tolerated dose · Phase-I study

Abstract
Aim: The aim of this phase-I study is to determine the maximum tolerated dose (MTD) of weekly gemcitabine in concurrent combination with a total radiation dose of 54 Gy in patients with pancreatic cancer. ***Methods:*** In all patients, a total dose of 54 Gy was delivered in 30 fractions of 1.8 Gy/day. Gross tumor volume and regional lymph nodes were included in the irradiated volume with a 1- to 1.5-cm margin. The doses of weekly gemcitabine were escalated from 100 mg/m^2 by increments of 50 mg/m^2. Dose-limiting toxicity (DLT) was defined as hematologic toxicity, prolonged grade-3 non-hematologic toxicity, and incompletion of the planned treatment. ***Results:*** Twenty-six patients entered the trial. From level 1 (100 mg/m^2) to level 4 (250 mg/m^2), no patient experienced DLT except for 1 patient at level 1. At level 5 (300 mg/m^2), 3 of the 5 patients met the DLT criteria. One patient developed severe pulmonary abscess, and the other 2 patients had hematologic DLT. The overall partial response rate was 29%, and the median survival time was 13.7 months. The first relapse occurred at the in-field primary site in 6 patients and at distant organs in 13 patients. ***Conclusion:*** The MTD of weekly gemcitabine was 250 mg/m^2 in the present chemoradiotherapy setting. The efficacy of this chemoradiotherapy regimen is currently being evaluated in the phase-II setting.

Introduction

Gemcitabine (2′-deoxy-2′-difluorocitidine), a purine analog, displays significant antitumor activity in a broad range of cancers. The clinical utility of gemcitabine in advanced pancreatic cancer is widely known by a randomized phase-III study, in which the palliative effect and survival benefit of gemcitabine was shown to be greater than that of 5-fluorouracil (5-FU) [1].

Patients with locally advanced nonresectable disease and without distant metastases are often treated with radiotherapy with or without concurrent use of chemotherapeutic agents with a radiosensitizing effect, including 5-FU [2]. Since the Gastrointestinal Study Group report-

KARGER
Fax +41 61 306 12 34
E-Mail karger@karger.ch
www.karger.com

1424–3903/06/0062–0109$23.50/0

Accessible online at:
www.karger.com/pan

Natsuo Oya, MD
Department of Radiation Oncology, Graduate School of Medical Sciences
Kumamoto University, 1-1-1 Honjo, Kumamoto 860-8556 (Japan)
Tel. +81 96 373 5520, Fax +81 96 362 4330
E-Mail n-oya@kaiju.medic.kumamoto-u.ac.jp

ed the survival advantage of concurrent chemoradiotherapy with 5-FU over radiotherapy alone, 5-FU-based chemoradiotherapy has been regarded as a standard strategy for locally advanced pancreatic cancer [3, 4].

Since the demonstration of the efficacy of gemcitabine as a potent radiosensitizing agent for human pancreatic cancer cells [5–7], many clinical trials have been undertaken to establish the use of gemcitabine-based chemoradiotherapy as an alternative strategy in treating locally advanced pancreatic cancer [8–17].

Although only a few studies have compared the outcome and toxicity of gemcitabine-based chemoradiotherapy with that of 5-FU-based chemoradiotherapy [13, 18], several preclinical studies and clinical phase-I/II studies have demonstrated gemcitabine as a promising agent in chemoradiotherapy for pancreatic cancer [8–12, 14–17].

However, the optimal use of gemcitabine remains controversial. A variety of recommended doses and schedules was reported in previous clinical studies, depending on patient background, disease status and, most importantly, on the concurrently used radiotherapy techniques, including radiation dose, fractionation, and the irradiated volume.

The main purpose of this phase-I trial was to determine the maximum tolerated dose (MTD) of weekly gemcitabine when concurrently combined with a fixed radiation dose of 54 Gy in patients with pancreatic cancer.

Methods and Materials

Patient Selection

This was a single-institutional phase-I study, approved by the institutional review board at Kyoto University Hospital. This study was carried out in accordance with the Helsinki Declaration. The entry criteria included patients with locally nonresectable pancreatic carcinoma with no evidence of distant metastases. Patients with limited para-aortic lymph node involvement at a level as low as the left renal vein were regarded as eligible. Postoperative patients with a positive surgical margin or with local recurrence after resection were also eligible, but only if they were to be treated exactly as the new cases.

Further eligibility included age between 20 and 75 years, ECOG performance status of 0–2, without preceding chemotherapy or radiotherapy, and without a history of another malignancy. Adequate bone marrow (white blood cell count 3,000–12.000/mm^3, platelet count >75,000/mm^3, and hemoglobin level >10 g/dl), renal function (blood urea nitrogen and creatinine within the normal limits), and hepatic function (aspartate aminotransferase (AST) and alanine aminotransferase (ALT) three times below the upper limit of normal) were also required. Written informed consent was provided by all patients.

Radiotherapy

The gross tumor volume (GTV) and the clinical target volume (CTV) were contoured on the planning CT scan with contrast at 5-mm intervals, where CTV was defined as the GTV plus a 5-mm margin in all directions as well as the potential para-aortic lymph node involvement between the celiac axis and the left renal vein. The planned target volume was determined by adding a horizontal 5-mm margin and a cephalocaudal 10-mm margin to the CTV, considering respiratory movement. The liver, kidneys and spinal cord were also contoured to calculate the dose volume histograms.

Patients were treated with 15-MV X-ray beams generated by a CLINAC-2100 (Varian, Palo Alto, Calif., USA). A total dose of 54 Gy was delivered in 30 daily fractions of 1.8 Gy over 6 weeks, using a three-field technique for the first 15 fractions and a dynamic arc conformal technique for the following 15 fractions [19–22]. The irradiation field was determined so that the entire planned target volume should be covered with the 95% isodose line. Thus, the total distance from the GTV edge to the field edge was 15–20 mm horizontally and 20–25 mm cephalocaudally. A sample of the summed dose distribution is illustrated in figure 1. The irradiation field was not reduced throughout the course of radiotherapy.

Gemcitabine Dose Escalation

Gemcitabine (Gemzar, Eli Lily, Indianapolis, Ind., USA) was reconstituted in saline and given as an intravenous infusion over 30 min, once a week during the 6-week radiotherapy, as shown in figure 2. If the radiotherapy period extended for over 6 weeks due to holidays, the schedule was modified keeping the proportion of 1 gemcitabine dose to 5 radiation doses.

The doses of weekly gemcitabine were escalated from 100 mg/m^2 by increments of 50 mg/m^2, each cohort consisting of 3–5 patients. Treatment-related acute toxicity was recorded according to the National Cancer Institute Common Toxicity Criteria. Blood samples were drawn twice a week during the radiotherapy period. Dose-limiting toxicity (DLT) was defined as: (1) hematologic toxicity of white blood cell count <1,000/mm^3, neutrophil count <500/mm^3, and platelet count <30,000/mm^3; (2) prolonged grade-3 nonhematologic toxicity except appetite loss and general malaise over 1 week, and (3) incompletion of the planned treatment (54 Gy and 6 gemcitabine doses) for any reason. Patients were evaluated for DLT until 2 months after the end of radiotherapy. The gemcitabine dose was escalated to the subsequent dose level when DLT was encountered in less than one third of the patients at a level. The MTD was defined as the dose level below that producing DLT in one third or more of the patients.

Response Evaluation and Patient Follow-Up

To evaluate tumor response and late toxicity, patient interview, physical examination, blood examination including relevant tumor markers, and CT imaging were performed at intervals of 4–8 weeks after completion of radiotherapy. The initial tumor response was judged within 3 months. As additional treatments, the protocol recommended 3 weekly doses of gemcitabine at 1,000 mg/m^2 every 28 days as long as possible, although it was in principle left to the discretion of the medical oncologists.

Statistics

In the assessment of the initial tumor response, a partial response (PR) was defined as a 30% reduction in the largest diameter of the primary lesions for at least 4 weeks: progressive disease (PD)

Table 1. Patient characteristics

Age, years	
40–49	2
50–59	6
60–69	14
≥70	4
Gender	
Male	17
Female	9
Performance status	
0	7
1	16
2	3
Tumor location	
Head	13
Body/tail	13
Tumor size, mm	
0–19	3
20–39	11
40–59	9
≥60	3
Disease status	
UICC stage III	17
UICC stage IV	5
Postoperative positive margin	2
Postoperative recurrence	2
Pretreatment CA 19-9 level, U/ml	
0–99	9
100–999	8
1,000–4,999	6
≥5,000	3

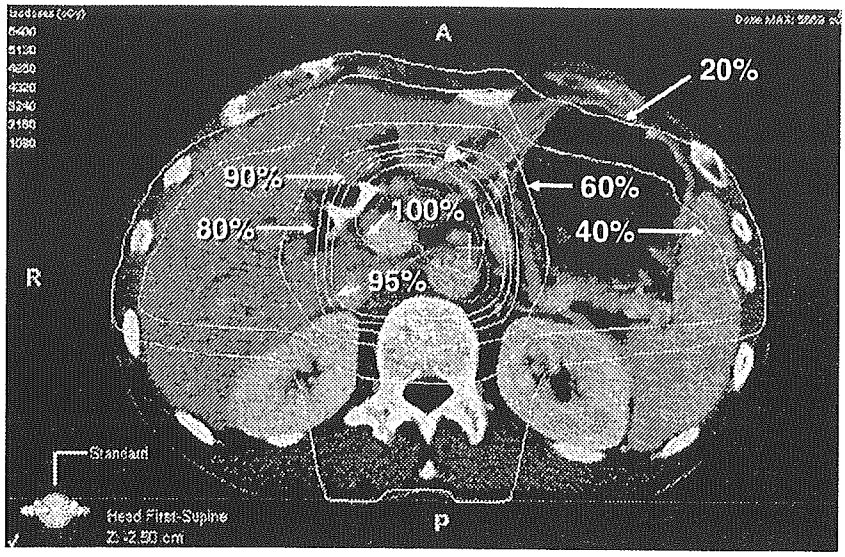

Fig. 1. Summed dose distribution by the half-and-half combination of the three-field and dynamic arc conformal irradiation techniques.

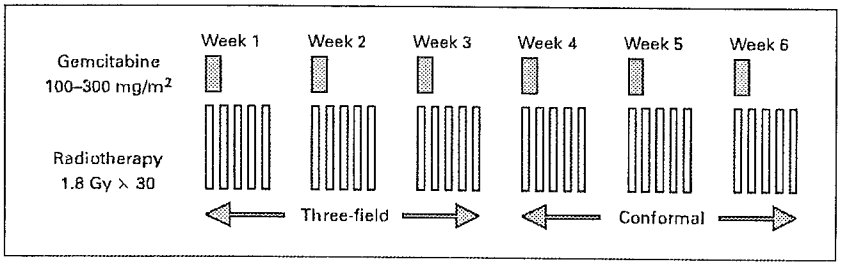

Fig. 2. Treatment schema.

was defined as a 20% increase in the largest diameter, and stable disease (SD) was defined as non-PR and non-PD, according to the Response Evaluation Criteria in Solid Tumors. Survival times were calculated from the day of the first fraction of radiotherapy using the Kaplan-Meier method, although this study was not designed for an outcome analysis.

Results

Patient Characteristics

Between July 2001 and March 2003, 26 patients (9 females and 17 males) entered the trial. The patient characteristics are summarized in table 1. The median patient age was 64 (range 41–75) years. The primary tumor location was the pancreatic head in 13 patients and the body/tail in 13.

The irradiated volume as the rectangular parallelepiped on the three-field technique ranged from 529 to 1,968 (median 1,002) ml. Of all 26 patients, 25 completed the planned radiotherapy, and their median overall treatment time was 44 (range 39–56) days, while 23 patients (88%) completed the planned chemoradiotherapy. Following the completion of the chemoradiotherapy, 18, 8 and 2 patients received ≥2, ≥5 and ≥10 courses of adjuvant gemcitabine, respectively.

Dose-Limiting Toxicity

Toxicity observed at each gemcitabine dose level is shown in table 2. At level 1 (100 mg/m^2, n = 5), 1 of the 5 patients suffered persistent grade-3 vomiting just after the first dose of gemcitabine, and no further gemcitabine could be administered. This patient completed radiother-

Table 2. Dose levels and toxicity

NCI-CTC grade	Patients	Leukopenia G0/G1/G2/G3/G4	Thrombocytopenia G0/G1/G2/G3/G4	Non-hematologic toxicity G0/G1/G2/G3/G4	Completion of 54 Gy and GEM ×6, yes/no	DLT-free yes/no
Level 1 (100 mg/m^2)	5	0/1/2/2/0	4/1/0/0/0	0/4/0/1/0	4/1	4/1
Level 2 (150 mg/m^2)	5	0/1/3/1/0	4/1/0/0/0	1/1/3/0/0	5/0	5/0
Level 3 (200 mg/m^2)	3	0/0/3/0/0	2/1/0/0/0	0/1/2/0/0	3/0	3/0
Level 4 (250 mg/m^2)	8	0/1/2/5/0	5/2/1/0/0	1/3/3/1/0	8/0	8/0
Level 5 (300 mg/m^2)	5	0/0/1/3/1	1/1/2/1/0	0/2/3/0/0	3/2	2/3

GEM = Gemcitabine; DLT = dose-limiting toxicity; NCI-CTC = National Cancer Institute Common Toxicity Criteria version 2.0.

apy alone to 54 Gy, but both the non-hematologic DLT and the DLT of the incompletion of the planned course of chemoradiotherapy were noted. None of the other 4 patients met the DLT criteria. At level 2 (150 mg/m^2, n = 5), level 3 (200 mg/m^2, n = 3) and level 4 (250 mg/m^2, n = 4), no patient experienced DLT. At level 5 (300 mg/m^2, n = 5), 3 of the 5 patients met the DLT criteria. One patient developed pulmonary abscess following continuous grade-3 leukopenia several days after the second dose of gemcitabine. After a 2-week interruption, radiotherapy alone was resumed without gemcitabine. Although it was not clear whether this complication should be regarded as treatment-related, it met at least one DLT criterion of the incompletion of the planned treatment. Another 2 patients at level 5 had hematologic DLT, one leukopenia, and the other thrombocytopenia. To confirm the tolerability of level 4, 4 patients were added to this cohort, and none of them experienced DLT. Thus, the MTD of weekly gemcitabine was determined to be 250 mg/m^2 in the present setting of chemoradiotherapy.

There was a tendency for the incidence of grade-3 leukopenia and grade-2 thrombocytopenia to increase according to the gemcitabine dose level, even though it was below the level of DLT. However, acute gastrointestinal toxicity did not seem to depend on the gemcitabine dose level.

Late Toxicity

In the 13 patients who survived longer than 6 months and underwent regular blood examinations, gastrointestinal, hepatic and renal late toxicity were assessed. Grade-3 gastrointestinal late toxicity was observed in 1 patient (at level 4), who developed hemorrhagic gastric ulcer 2 and 5 months after completion of chemoradiotherapy. No grade-2–4 hepatic or renal late toxicity was experienced. Grade-1 hepatic toxicity (AST/ALT <2.5-fold the upper normal limit) and grade-1 renal toxicity (creatinine <2.0 mg/dl) was observed in 3 (all at level 1) and 2 patients (1 at level 1 and 1 at level 3), respectively. To evaluate the influence of the irradiated dose of these organs on toxicity, a dose volume histogram (DVH) was analyzed for all 13 patients. The median %V30Gy of the liver, %V25Gy of the right kidney and %V25Gy of the left kidney were 11.4% (range 1.6–34.4%), 9.3% (range 3.1–18.4%) and 8.3% (range 0.2–26.6%), respectively. There was no relationship between the DVH profile and toxicity, or between the gemcitabine dose and toxicity.

Clinical Response

For the 24 patients who had measurable tumor, follow-up CT studies were obtained at least once within 3 months after treatment to determine the initial tumor response. Radiologic SD was observed in 17, PD in 1 (at level 1), and PR in 7 (1 at level 1, 1 at level 2, 1 at level 3, 2 at level 4 and 2 at level 5) patients. A PR case is shown in figure 3. The overall PR rate was 29%. Of the 23 patients whose pretreatment CA 19-9 value was above the normal limit, 20 (87%) showed a decrease within 3 months after treatment.

The overall survival curve for the 24 patients excluding the 2 postoperative cases is shown in figure 4. Median survival time (MST) was 13.7 months, where the median follow-up time of the survivors was 11 months. The first relapse occurred at the in-field primary site in 6 patients and at distant organs in 13 patients (6 peritoneal, 5 liver, 1 skin and 1 lung metastasis).

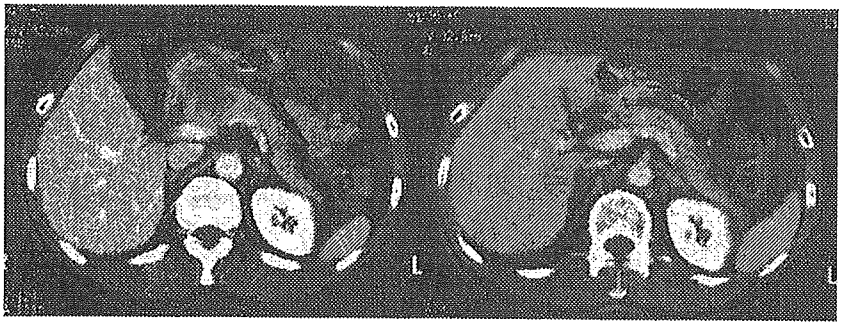

Fig. 3. Pre- and post-treatment CT scans in a patient achieving a partial response (PR).

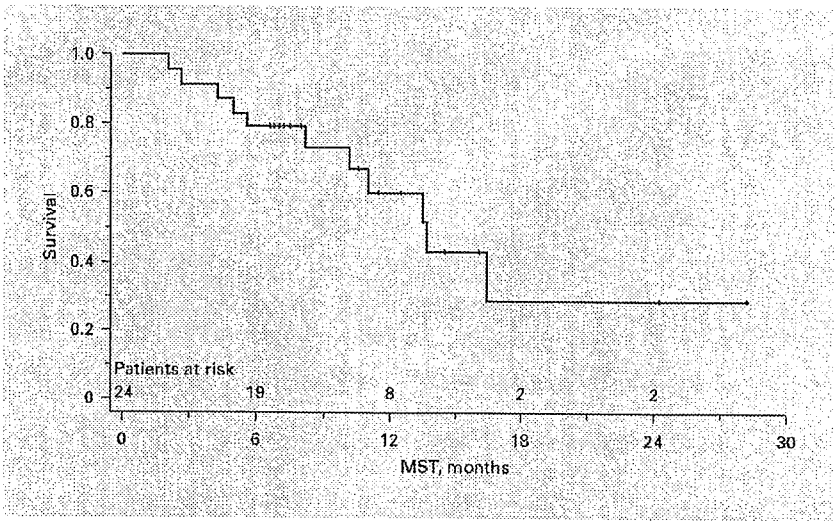

Fig. 4. Overall survival for the 24 patients with gross tumor. Median survival time (MST) was 13.7 months.

Discussion

When gemcitabine is used as a single agent for patients with advanced pancreatic cancer, the standard weekly dose is around 1,000 mg/m^2 [1, 23]. On the other hand, a total radiation dose of at least 50–60 Gy may be necessary to achieve local control, if radiosensitization is not considered [3]. Considering both the radioresistant and metastasis-prone nature of pancreatic cancer, the concurrent combination of full-dose radiotherapy and full-dose gemcitabine should produce the best outcome. However, this appears to be too toxic in clinical practice [10, 11].

A phase-I study of chemoradiotherapy with a fixed standard dose of gemcitabine (1,000 mg/m^2 gemcitabine on days 1, 8 and 15 of every 28 days) was undertaken to determine the MTD of concurrent 15-fractionated radiotherapy by McGinn et al. [9]. The radiation dose was escalated from 24 Gy in 1.6-Gy fractions to 42 Gy in 2.8-Gy fractions, concluding that 36 Gy in 2.4-Gy fractions was to be recommended [9]. This approach had the advantage that the systemic antitumor effect of gemcitabine as well as the radiosensitizing effect was expected even during the radiotherapy period, although the radiation dose given was considerably low for tumor control.

Several phase-I studies have been performed to determine the MTD of concurrent gemcitabine with a fixed radiation dose fractionation. Two independent studies of conventional radiotherapy with twice-weekly gemcitabine were reported by Blackstock et al. [8] and Pipas et al. [15]. The MTD of gemcitabine was shown to be as low as 40 and 50 mg/m^2, respectively, in combination with a total dose of 50.4 Gy in 1.8-Gy fractions [8, 15]. Toxicity seen even at considerably low dose levels of gemcitabine may suggest its great efficacy as a pure radiosensitizer, if administered frequently with radiotherapy.

Phase-I studies of short-course radiotherapy with weekly gemcitabine have been reported by Crane et al. [12] and Wolff et al. [16]. The former showed the high

incidence (24%) of severe acute toxicity in patients treated with 200–500 mg/m^2 gemcitabine in combination with a total dose of 30–33 Gy in 3-Gy fractions [12]. The latter showed that the MTD of weekly gemcitabine was 350 mg/m^2 with a total dose of 30 Gy in 3-Gy fractions, the gemcitabine dose being decreased from the starting dose level of 400 mg/m^2 [16]. Short-course chemoradiotherapy with a hypofractionated schedule has the advantage that the patients could be transferred earlier to intense systemic therapy. However, both of these reports described difficulty in combining modest doses of weekly gemcitabine and daily 3-Gy fractions of irradiation to the upper abdomen.

Several phase-I and phase-II studies of conventional radiotherapy with weekly gemcitabine have also been reported. Ikeda et al. [10] showed an MTD of 250 mg/m^2 with a total dose of 50.4 Gy in 1.8-Gy fractions. Poggi et al. [11] showed the MTD of 440 mg/m^2 with a total dose of 54–55.8 Gy in 1.8-Gy fractions. Epelbaum et al. [14] reported that chemoradiotherapy with weekly gemcitabine of 400 mg/m^2 and a total dose of 50.4 Gy in 1.8-Gy fractions, following a standard-dose of gemcitabine for 7 weeks as an induction phase, was well tolerated.

The feasibility of chemoradiotherapy with gemcitabine plus another agent, including 5-FU, mitomycin C, cisplatin and paclitaxel, has also been evaluated in various regimens. Talamonti et al. [24] reported the unexpected early toxicity of the concurrent chemoradiotherapy with a total radiation dose of 59.4 Gy and gemcitabine plus prolonged infusion of 5-FU. Kornek et al. [25] showed the MTD of weekly 24-hour continuous infusion of gemcitabine was 130 mg/m^2 combined with a dose of mitomycin C of 8 mg/m^2 and a total radiation dose of 45 Gy. In addition, the feasibility of chemoradiotherapy with gemcitabine and cisplatin was reported by Martenson et al. [26] and Brunner et al. [27]. The former showed that twice-weekly gemcitabine at 30 mg/m^2 and twice-weekly cisplatin at 10 mg/m^2 with concurrent radiotherapy of 50.4 Gy was acceptable [26], and the latter showed that weekly gemcitabine at 300 mg/m^2 and 10 daily doses of cisplatin at 20 mg/m^2 with concurrent radiotherapy of 55.8 Gy was recommendable [27]. Safran et al. [28] reported the feasibility of chemoradiotherapy with a total radiation dose of 50.4 Gy and weekly gemcitabine at 75 mg/m^2 plus weekly paclitaxel at 40 mg/m^2.

The current study was designed as an orthodox phase-I trial of gemcitabine dose escalation with concurrent conventional radiotherapy at a total dose of 54 Gy in 1.8-Gy fractions. The MTD was shown to be 250 mg/m^2. It is interesting that the current study showed the same MTD as an independent Japanese phase-I study, although the total radiation dose, irradiation techniques used, and the DLT were considerably different [10]. In the current study, 3 of the 5 patients at level 5 (300 mg/m^2) met the DLT criteria. The DLT was mainly hematologic toxicity, including 1 patient who developed pulmonary abscess after grade-3 leukopenia, while non-hematologic toxicity did not depend on the gemcitabine dose level. It is notable that gastrointestinal DLT was not uncommon in most previous phase-I studies, particularly in the setting of twice-weekly gemcitabine or short-course radiotherapy [15, 16, 26]. In addition, all 8 patients at level 4 (250 mg/m^2) completed the planned chemoradiotherapy without DLT, suggesting good compliance at this dose level.

Overall, the late toxicity observed in the current study seemed to be acceptable. We employed a half-and-half combination of the three-field and dynamic arc conformal irradiation techniques, according to previous studies at our institute [19–22], considering the balance between the DVHs of liver and kidneys. No grade-2 hepatic or renal toxicity was encountered, suggesting that this irradiation technique is safe also with concurrent gemcitabine. Grade-3 gastrointestinal late toxicity occurred in only 1 patient, who developed hemorrhagic gastric ulcer and was treated conservatively. The incidence of late gastrointestinal toxicity, however, might have been under-evaluated, because endoscopic examination was performed only for symptomatic patients.

The overall PR rate of the current study was 29%, which is comparable to those in the previously published phase-I and phase-II studies of gemcitabine-based chemoradiotherapy (7–40%) [5, 10, 14, 16, 17, 25, 27–29]. The calculated MST of 13.7 months appeared to be comparable to those in the previous studies of gemcitabine-based chemoradiotherapy, which treated patients with locally advanced nonresectable pancreatic cancer and without distant metastases (6–14.5 months) [11–14, 16, 17, 25–27, 30], and better than those in 5-FU-based chemoradiotherapy [3, 13]. The recurrence pattern differed among the reports. One report showed that the local progression rate at 9 months was 70% [12], and another showed that 18 of 19 recurrences were distant metastases [11]. In the current study, the majority (68%) of the first recurrence occurred at a distant organ, suggesting the considerable local antitumor effect and the limitations of the systemic effect of this treatment regimen.

At present, many unsolved issues exist in treating locally advanced pancreatic cancer, including the optimal dose-fractionation of radiotherapy, radiation treatment volume, combined concurrent or sequential chemother-

apy, and even whether chemoradiotherapy is better than systemic chemotherapy alone [31]. On the other hand, more recently, several novel approaches in gemcitabine-based chemoradiotherapy have been attempted including combination with celecoxib (a cyclooxygenase-2 inhibitor) [32], amifostine (WR-2721) [29], and intensity-modulated radiotherapy (IMRT) [33, 34]. Therefore, further information on the long-term outcome and late toxicity by phase-II or phase-III trials are being anticipated to establish the optimal strategy.

In conclusion, the MTD of weekly gemcitabine was 250 mg/m^2, when combined with a total radiation dose of 54 Gy in 1.8-Gy fractions. The efficacy of this chemoradiotherapy regimen is currently being evaluated in the phase-II setting.

References

1 Burris HA 3rd, Moore MJ, Andersen J, Green MR, Rothenberg ML, Modiano MR, Cripps MC, Portenoy RK, Storniolo AM, Tarassoff P, Nelson R, Dorr FA, Stephens CD, Von Hoff DD: Improvements in survival and clinical benefit with gemcitabine as first-line therapy for patients with advanced pancreas cancer: a randomized trial. J Clin Oncol 1997;15:2403–2413.

2 Balart J, Capella G, de los Inocentes RM, de Andres J, Ares C, Craven-Bartle J, Lluis F: Treatment with 5-fluorouracil enhances radiosensitivity of the human pancreatic cancer cell line MiaPaCa-2. Pancreatology 2002;2:40–45.

3 Moertel CG, Frytak S, Hahn RG, O'Connell MJ, Reitemeier RJ, Rubin J, Schutt AJ, Weiland LH, Childs DS, Holbrook MA, Lavin PT, Livstone E, Spiro H, Knowlton A, Kalser M, Barkin J, Lessner H, Mann-Kaplan R, Ramming K, Douglas HO Jr, Thomas P, Nave H, Bateman J, Lokich J, Brooks J, Chaffey J, Corson JM, Zamcheck N, Novak JW: Therapy of locally unresectable pancreatic carcinoma: a randomized comparison of high dose (6000 rads) radiation alone, moderate dose radiation (4000 rads + 5-fluorouracil), and high dose radiation + 5-fluorouracil: The Gastrointestinal Tumor Study Group. Cancer 1981;48:1705–1710.

4 Fisher BJ, Perera FE, Kocha W, Tomiak A, Taylor M, Vincent M, Bauman GS: Analysis of the clinical benefit of 5-fluorouracil and radiation treatment in locally advanced pancreatic cancer. Int J Radiat Oncol Biol Phys 1999; 45:291–295.

5 Lawrence TS, Chang EY, Hahn TM, Hertel LW, Shewach DS: Radiosensitization of pancreatic cancer cells by 2′,2′-difluoro-2′-deoxycytidine. Int J Radiat Oncol Biol Phys 1996; 34:867–872.

6 Shewach DS, Lawrence TS: Radiosensitization of human solid tumor cell lines with gemcitabine. Semin Oncol 1996;23(suppl 10):65–71.

7 Weiss C, Grabenbauer GG, Sauer R, Distel L: Significant increase in residual DNA damage as a possible mechanism of radiosensitization by gemcitabine. Strahlenther Onkol 2003;179: 93–98.

8 Blackstock AW, Bernard SA, Richards F, Eagle KS, Case LD, Poole ME, Savage PD, Tepper JE: Phase I trial of twice-weekly gemcitabine and concurrent radiation in patients with advanced pancreatic cancer. J Clin Oncol 1999; 17:2208–2212.

9 McGinn CJ, Zalupski MM, Shureiqi I, Robertson JM, Eckhauser FE, Smith DC, Brown D, Hejna G, Strawderman M, Normolle D, Lawrence TS: Phase I trial of radiation dose escalation with concurrent weekly full-dose gemcitabine in patients with advanced pancreatic cancer. J Clin Oncol 2001;19:4202–4208.

10 Ikeda M, Okada S, Tokuuye K, Ueno H, Okusaka T: A phase I trial of weekly gemcitabine and concurrent radiotherapy in patients with locally advanced pancreatic cancer. Br J Cancer 2002;86:1551–1554.

11 Poggi MM, Kroog GS, Russo A, Muir C, Cook J, Smith J, Mitchell JB, Herscher LL: Phase I study of weekly gemcitabine as a radiation sensitizer for unresectable pancreatic cancer. Int J Radiat Oncol Biol Phys 2002;54:670–676.

12 Crane CH, Janjan NA, Evans DB, Wolff RA, Ballo MT, Milas L, Mason K, Charnsangavej C, Pisters PW, Lee JE, Lenzi R, Vauthey JN, Wong A, Phan T, Nguyen Q, Abbruzzese JL: Toxicity and efficacy of concurrent gemcitabine and radiotherapy for locally advanced pancreatic cancer. Int J Pancreatol 2001;29:9–18.

13 Li CP, Chao Y, Chi KH, Chan WK, Teng HC, Lee RC, Chang FY, Lee SD, Yen SH: Concurrent chemoradiotherapy treatment of locally advanced pancreatic cancer: gemcitabine versus 5-fluorouracil, a randomized controlled study. Int J Radiat Oncol Biol Phys 2003;57: 98–104.

14 Epelbaum R, Rosenblatt E, Nasrallah S, Faraggi D, Gaitini D, Mizrahi S, Kuten A: Phase II study of gemcitabine combined with radiation therapy in patients with localized, unresectable pancreatic cancer. J Surg Oncol 2002; 81:138–143.

15 Pipas JM, Mitchell SE, Barth RJ Jr, Vera-Gimon R, Rathmann J, Meyer LP, Wagman RS, Lewis LD, McDonnell C, Colacchio TA, Perez RP: Phase I study of twice-weekly gemcitabine and concomitant external-beam radiotherapy in patients with adenocarcinoma of the pancreas. Int J Radiat Oncol Biol Phys 2001;50: 1317–1322.

16 Wolff RA, Evans DB, Gravel DM, Lenzi R, Pisters PW, Lee JE, Janjan NA, Charnsangavej C, Abbruzzese JL: Phase I trial of gemcitabine combined with radiation for the treatment of locally advanced pancreatic adenocarcinoma. Clin Cancer Res 2001;7:2246–2253.

17 de Lange SM, van Groeningen CJ, Meijer OW, Cuesta MA, Langendijk JA, van Riel JM, Pinedo HM, Peters GJ, Meijer S, Slotman BJ, Giaccone G: Gemcitabine-radiotherapy in patients with locally advanced pancreatic cancer. Eur J Cancer 2002;38:1212–1217.

18 Crane CH, Abbruzzese JL, Evans DB, Wolff RA, Ballo MT, Delclos M, Milas L, Mason K, Charnsangavej C, Pisters PW, Lee JE, Lenzi R, Vauthey JN, Wong AB, Phan T, Nguyen Q, Janjan NA: Is the therapeutic index better with gemcitabine-based chemoradiation than with 5-fluorouracil-based chemoradiation in locally advanced pancreatic cancer? Int J Radiat Oncol Biol Phys 2002;52:1293–1302.

19 Kokubo M, Nishimura Y, Shibamoto Y, Sasai K, Kanamori S, Hosotani R, Imamura M, Hiraoka M: Analysis of the clinical benefit of intraoperative radiotherapy in patients undergoing macroscopically curative resection for pancreatic cancer. Int J Radiat Oncol Biol Phys 2000;48:1081–1087.

20 Kokubo M, Nishimura Y, Shibamoto Y, Sasai K, Hosotani R, Imamura M, Hiraoka M: Concurrent chemoradiotherapy combined with intraoperative radiotherapy for locally advanced pancreatic cancer: a feasibility study. Oncol Rep 2000;7:773–776.

21 Kokubo M, Nishimura Y, Nagata Y, Mizowaki T, Yamamoto M, Kanamori S, Katakura Y, Hiraoka M, Abe M: Dose-volume histogram analysis of external-beam irradiation combined with IORT for unresectable pancreatic cancer. Front Radiat Ther Oncol 1997;31: 177–180.

22 Nishimura Y, Hosotani R, Shibamoto Y, Kokubo M, Kanamori S, Sasai K, Hiraoka M, Ohshio G, Imamura M, Takahashi M, Abe M: External and intraoperative radiotherapy for resectable and unresectable pancreatic cancer: analysis of survival rates and complications. Int J Radiat Oncol Biol Phys 1997;39:39–49.

23 Casper ES, Green MR, Kelsen DP, Heelan RT, Brown TD, Flombaum CD, Trochanowski B, Tarassoff PG: Phase II trial of gemcitabine (2,2'-difluorodeoxycytidine) in patients with adenocarcinoma of the pancreas. Invest New Drugs 1994;12:29–34.

24 Talamonti MS, Catalano PJ, Vaughn DJ, Whittington R, Beauchamp RD, Berlin J, Benson AB 3rd: Eastern Cooperative Oncology Group Phase I trial of protracted venous infusion fluorouracil plus weekly gemcitabine with concurrent radiation therapy in patients with locally advanced pancreas cancer: a regimen with unexpected early toxicity. J Clin Oncol 2000;18:3384–3389.

25 Kornek GV, Potter R, Selzer E, Schratter A, Ulrich-Pur H, Rogy M, Kraus G, Scheithauer W: Combined radiochemotherapy of locally advanced unresectable pancreatic adenocarcinoma with mitomycin C plus 24-hour continuous infusional gemcitabine. Int J Radiat Oncol Biol Phys 2001;49:665–671.

26 Martenson JA, Vigliotti AP, Pitot HC, Geeraerts LH, Sargent DJ, Haddock MG, Ghosh C, Keppen MD, Fitch TR, Goldberg RM: A phase I study of radiation therapy and twice-weekly gemcitabine and cisplatin in patients with locally advanced pancreatic cancer. Int J Radiat Oncol Biol Phys 2003;55:1305–1310.

27 Brunner TB, Grabenbauer GG, Klein P, Baum U, Papadopoulos T, Bautz W, Hohenberger W, Sauer R: Phase I trial of strictly time-scheduled gemcitabine and cisplatin with concurrent radiotherapy in patients with locally advanced pancreatic cancer. Int J Radiat Oncol Biol Phys 2003;55:144–153.

28 Safran H, Dipetrillo T, Iannitti D, Quirk D, Akerman P, Cruff D, Cioffi W, Shah S, Ramdin N, Rich T: Gemcitabine, paclitaxel, and radiation for locally advanced pancreatic cancer: a phase I trial. Int J Radiat Oncol Biol Phys 2002;54:137–141.

29 Yavuz AA, Aydin F, Yavuz MN, Ilis E, Ozdemir F: Radiation therapy and concurrent fixed dose amifostine with escalating doses of twice-weekly gemcitabine in advanced pancreatic cancer. Int J Radiat Oncol Biol Phys 2001; 51:974–981.

30 Okusaka T, Ito Y, Ueno H, Ikeda M, Takezako Y, Morizane C, Kagami Y, Ikeda H: Phase II study of radiotherapy combined with gemcitabine for locally advanced pancreatic cancer. Br J Cancer 2004;91:673–677.

31 Wenz F, Tiefenbacher U, Fuss M, Lohr F: Should patients with locally advanced, nonmetastatic carcinoma of the pancreas be irradiated? Pancreatology 2003;3:359–366.

32 Crane CH, Mason K, Janjan NA, Milas L: Initial experience combining cyclooxygenase-2 inhibition with chemoradiation for locally advanced pancreatic cancer. Am J Clin Oncol 2003;26:S81–S84.

33 Crane CH, Antolak JA, Rosen II, Forster KM, Evans DB, Janjan NA, Charnsangavej C, Pisters PW, Lenzi R, Papagikos MA, Wolff RA: Phase I study of concomitant gemcitabine and IMRT for patients with unresectable adenocarcinoma of the pancreatic head. Int J Gastrointest Cancer 2001;30:123–132.

34 Bai YR, Wu GH, Guo WJ, Wu XD, Yao Y, Chen Y, Zhou RH, Lu DQ: Intensity modulated radiation therapy and chemotherapy for locally advanced pancreatic cancer: results of feasibility study. World J Gastroenterol 2003; 9:2561–2564.

World Journal of Surgery

Published Online: 21 January 2006

World J Surg (2006) 30: 1–8
DOI: 10.1007/s00268-005-0165-z

Clinical Significance of Focal Adhesion Kinase in Resectable Pancreatic Cancer

Kenichiro Furuyama, MD, Ryuichiro Doi, MD, Tomohiko Mori, MD, Eiji Toyoda, MD, Daisuke Ito, MD, Kazuhiro Kami, MD, Masayuki Koizumi, MD, Atsushi Kida, MD, Yoshiya Kawaguchi, MD, Koji Fujimoto, MD

Department of Surgery and Surgical Basic Science, Kyoto University, 54 Shogoinkawaracho, Sakyo, Kyoto 606-8507, Japan

Abstract

Focal adhesion kinase (FAK) is a non-receptor, cytoplasmic protein tyrosine kinase that is involved in the regulation of cellular signaling, migration, apoptosis, and cell cycle progression. Previous reports have shown that FAK is expressed in various kinds of cancer tissues and cancer cell lines; however, no information is available about human pancreatic carcinoma specimens. Tissue such specimens were obtained from 50 patients who underwent pancreatic resection for pancreatic invasive ductal carcinoma at our institute from 1996 to 2002. Immunohistochemical analysis of FAK was performed in the resected specimens. Focal adhesion kinase expression in seven human pancreatic cancer cell lines was analyzed by reverse transcription polymerase chain reaction (PCR) analysis and Western blot analysis. Focal adhesion kinase expression was detected in 24 of 50 cases (48%). There was a statistically significant correlation between FAK expression and tumor size ($P = 0.004$), although FAK expression did not significantly correlate with other factors such as tumor histological grade, lymph node metastasis, distant metastasis, histological stage, and overall survival. Reverse transcription PCR analysis and Western blot analysis showed that FAK was expressed in all seven pancreatic cancer cell lines. Focal adhesion kinase expression was not directly related to clinicopathological factors except tumor size in pancreatic carcinoma. Focal adhesion kinase expression may not be a prognostic marker for pancreatic cancer patients.

Pancreatic ductal adenocarcinoma is one of the most aggressive tumors associated with high morbidity and mortality. It is the fourth leading cause of cancer death, accounting for an estimated 30,700 new cases and an estimated 30,000 deaths annually in the United States. This malignancy is highly fatal with an overall 5-year survival rate of less than 5% even after aggressive surgical treatment.

Focal adhesion kinase (FAK) is a non-receptor cytoplasmic protein tyrosine kinase that is localized to cellular focal adhesions; it was originally isolated from v-src–transformed chick embryo fibroblasts.[1] Focal adhesion kinase protein plays physiologically important roles in the regulation of cellular signaling, adhesion, migration, apoptosis, and cell cycle progression.[2–4] In addition, FAK expression is elevated in a number of different tumors including breast, colon, thyroid, head and neck, ovarian, liver, and esophageal cancers;[5–9] however, no information is available on FAK expression in pancreatic cancer. The present study was conducted to determine the relationship between FAK expression and the clinicopathological factors in pancreatic adenocarcinoma.

Correspondence to: Ryuichiro Doi, MD, Department of Surgery and Surgical Basic Science, Kyoto University, 54 Shogoinkawaracho, Sakyo, Kyoto 606-8507, Japan, e-mail: doir@kuhp.kyoto-u.ac.jp

MATERIALS AND METHODS

Tissue Samples

Formalin-fixed paraffin-embedded tissue specimens were obtained from 50 patients with pancreatic invasive ductal carcinoma confirmed by histopathologic diagnosis who underwent pancreatic resection at the Department of Surgery and Surgical Basic Science, Kyoto University, between 1996 and 2002. Patients with other pancreatic malignancies such as intraductal papillary mucinous neoplasm, acinar cell carcinoma, or endocrine tumors were excluded. The patients included in this study were 31 men and 19 women, whose ages ranged from 45 to 79 years (64.3 ± 8.3 years [mean ± SD]). Tumor specimens were collected after obtaining the patients' informed consent in accordance with institutional guidelines. Tissue samples were fixed with 4% paraformaldehyde, embedded in paraffin, and cut into 4-μm-thick sections.

Immunohistochemistry

All slides were deparaffinized using xylene, 100% ethanol, and 90% ethanol, followed by a thorough deionized water wash. During heat-induced epitope recovery, sections were kept at 95°C while submerged in Target Retrieval Solution (S3307; DAKO Cytomation, Kyoto, Japan) for 45 minutes, then cooled for 20 minutes at room temperature followed by a twice deionized water wash. To quench endogenous peroxidase activity, samples were blocked in 3% hydrogen peroxide in methanol for 15 minutes at room temperature and then washed in Tris buffered saline buffer containing 0.05% Tween 20 (TBST). Sections were blocked in normal goat serum for 30 minutes, then blown off and incubated at 4°C overnight with mouse antihuman FAK antibody (05-537; Upstate Biotechnology, Waltham, MA) at a dilution of 1:200 in Dako diluent (DAKO Cytomation, Kyoto, Japan). The sections were washed in TBST and then incubated with biotinylated goat anti-mouse IgG at a dilution of 1:300 (DAKO Cytomation) for 60 minutes at room temperature. The slides were washed in TBST, and then horseradish peroxidase-conjugated streptavidin at a 1:300 dilution (DAKO Cytomation) was applied for 20 minutes incubation. The chromogenic reaction was performed with DAB, toned with the DAB + substrate solution (K3468; DAKO Cytomation) for 5 minutes. Slides were counterstained with Mayer hematoxylin for 5 minutes before they were dehydrated and cover-slipped with permanent mounting medium (Richard-Allan Scientific, Kalamazoo, MI). Negative controls were prepared by substituting normal mouse serum for primary antibody, and no detectable staining was evident.

Immunohistochemical Scoring

The expression of FAK was evaluated independently by two investigators (K.F. and R.D.) in blinded fashion. For each tissue, FAK expression was examined on a scoring system that measured intensity (0, none; 1, borderline; 2, weak; 3, moderate; 4, strong) and the proportion of positively stained cells among cancer cells (0 = none; 1 = 1%–49%; 2 = 50%–100%). Scores between investigators were averaged, and a mean scored was calculated for each sample. The staining intensity score was multiplied by the score of positively stained cells to obtain the overall score. The specimens with a staining intensity score greater than 2 were regarded as positive expression of FAK.

Cell Lines

Pancreatic cancer cell lines, AsPC-1, BxPC-3, CFPAC-1, HPAC, MIAPaCa-2, PANC-1, and Suit-2, were cultured as monolayers in the appropriate medium[10] supplemented with 10% fetal bovine serum, 100 U/ml penicillin, and 100 μg/ml streptomycin and maintained in a 5% humidified CO2 atmosphere at 37°C, and the medium was replaced as needed.

Western Blot Analysis

To perform sodium dodecylsulfate-polyacrylamide gel electrophoresis (SDS-PAGE) and Western blot analysis for FAK expression, cells were plated onto 100-mm dishes and grown to 80% confluence. Cells were harvested by scraping on ice and lysed for 60 minutes in phosphorylation-inhibitory RIPA buffer containing 50 mM Hepes (pH 7.0), 250 mM NaCl, 0.1% Nonidet P-40, 1 mM phenylmethylsulfonyl fluoride (PMSF), and 20 μg/ml gabexate mesilate, and then they were sonicated for 20 seconds. Total extracts were cleaned by centrifugation at 12,000 rpm for 10 minutes at 4°C and the supernatants were collected. Protein concentrations were measured using BCA Protein Assay Reagents (Pierce, Rockford, IL). The lysates were re-suspended in the same volume of the gel loading buffer, which contained 50 mM Tris-HCl (pH 6.7), 4% SDS, 0.02% bromophenol blue, 20% glycerol, and 4% 2-mercaptoethanol, and then boiled at 95°C for 3 minutes. The extracted protein was subjected to

Western blotting, as previously described.[10] In brief, 30-microgram aliquots that were taken from the total quantity of protein were size-fractionated to a single dimension by SDS-PAGE (6% sodium dodecylsulfate gel) and transblotted to 0.45-μm polyvinylidene difluoride membrane (Bio-Rad, Richmond, CA) in a semi-dry electroblot apparatus (Bio-Rad). Membranes were blocked overnight at 4°C in Tris-buffered saline (TBS) containing 5% bovine serum albumin and 0.1% Tween 20. The membrane was probed with anti-FAK monoclonal antibody at 1:1000 dilution (05-537; Upstate Biotechnology, Waltham, MA), anti-FAK rabbit polyclonal phosphospecific antibody at 1:500 dilution (44-624; Biosource, Camarillo, CA) or anti-beta-actin monoclonal antibody at 1:5000 dilution (A5441; Sigma, St. Louis, MO). Anti-beta-actin antibody served as the internal control. The membrane was washed with several changes of medium. The proteins were visualized by enhanced chemiluminescence regents (Amersham, Buckinghamshire, UK) according to the manufacturer's instructions using goat anti-mouse horseradish peroxidase-conjugated IgG at 1:2000 dilution (62-6520; ZYMED, San Francisco, CA) or goat anti-rabbit horseradish peroxidase-conjugated IgG at 1:2000 (62-6120; ZYMED). Membranes were exposed to x-ray film for 20–60 seconds.

Reverse-transcriptional PCR

Total cellular RNA was extracted using TRIZOL Reagent (Life Technologies, Rockville, MD), and cDNA was synthesized by random priming from 1 μg of total RNA using a first-strand cDNA synthesis kit (Pharmacia Biotech, North Peapack, NJ) according to the manufacturer's instructions. Primer sequences used are listed as forward then reverse 5′ to 3′. Focal adhesion kinase primers 5′ aatacggcgatcatactggg3′ and 5′catgccttgcttttcg ctgt3′ amplify a product of 620 base pairs, and beta-actin primers 5′ggcatcgtgatggactccg3′ and 5′gctggaaggt ggacagcg3′ amplify a product of 612 base pairs. The PCR was carried out with a mixture of cDNA (derived from 100 ng of RNA), 0.2 μM each of the sense and antisense primers, 0.2 μM of deoxynucleotide triphosphate, and 2.5 U Taq DNA polymerase in reaction buffer (TaKaRa, Kyoto, Japan) with a final volume of 50 μl. The PCR reactions were performed as follows; 1 cycle of 94°C for 5 minutes; then 40 cycles of 94°C for 30 seconds, 52°C for 30 seconds, 72°C for 30 seconds, and finally 1 cycle of 72°C for 7 minutes in a thermal cycler (Gene Amp PCR system 2400; PE Applied Biosystems, Foster City, CA). Products of amplification were separated on 1% agarose gel and photographed after ethidium bromide staining.

Statistical Analysis

Clinicopathological characteristics were compared with FAK expression (positive and negative) using the chi-squared test or the Fisher's exact probability test. The Kaplan-Meier method was used to calculate the survival curves, and the log-rank test was performed to compare differences in the survival rates of patients. All analyses were done using Stat View software (version J-4.5; Abacus Concepts, Berkeley, CA). A probability value < 0.05 was considered statistically significant.

RESULTS

FAK mRNA Expression and FAK Protein Expression in Pancreatic Cancer Cell Lines

The mRNA expression of FAK in seven pancreatic cancer cell lines (AsPC-1, BxPC-3, CFPAC-1, HPAC, MIAPaCa-2, PANC-1, and Suit-2) derived from human pancreatic adenocarcinoma was tested with reverse-transcriptional PCR analysis. Focal adhesion kinase mRNA was detected in all seven cell lines (Fig. 1).

Focal adhesion kinase protein expression levels in pancreatic cancer cell lines were evaluated by Western blot analysis (Fig. 2). In all seven pancreatic cancer cell lines the FAK protein was detected as a single band corresponding to the molecular size of 125 kDa. The FAK expression at the protein level was similar among seven cell lines.

FAK Phosphorylation at Tyrosin 397 in Pancreatic Cancer Cell Lines

There are six tyrosin phosphorylation sites in the FAK catalytic domain. The major site of autophosphorylation, tyrosin 397, is a docking site for the SH2 domains of a number of proteins, including the Src family of tyrosin kinase[11], phosphatidylinositol 3′-kinase[12], phospholipase C[13], and Grb7[14]. To investigate the catalytic activity of FAK in each cell line, immunoblotting with anti-FAK [pY397] was performed (Fig. 3). The level of FAK phosphorylation at tyrosine 397 was not changed by serum in all cell lines.

Expression of FAK in Pancreatic Cancer and Normal Pancreatic Tissues

Focal adhesion kinase expression in pancreatic tissues was investigated by immunohistochemical analy-

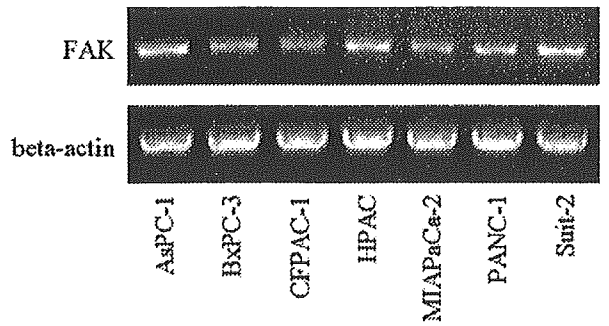

Figure 1. FAK mRNA expression in pancreatic cancer cell lines. Reverse-transcriptional PCR analysis showed the mRNA expression of FAK in seven cell lines derived from pancreatic adenocarcinoma. FAK mRNA expression was detected in all seven cell lines.

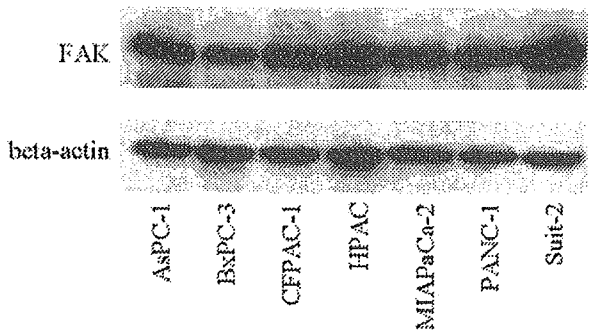

Figure 2. Expression of FAK protein in pancreatic cancer cell lines. FAK was detected in pancreatic cancer cell lines by Western blot. The FAK expression levels were similar among cell lines.

Table 1.
Clinical profile of patients with pancreatic cancer

	FAK-positive n = 24 (48%)	FAK-negative n = 26 (52%)
Age	64.1 ± 8.5	64.4 ± 8.2
Sex	15	16
male	15	16
female	9	10

sis, and FAK staining was identified not only in cancer cells but also in normal ductal cells (Fig. 4). In normal pancreatic tissue, FAK staining was observed strongly in the cytoplasm of ductal cells, faintly in islet cells, but not in acinar cells. In pancreatic cancer tissue, FAK was expressed in the cytoplasm and on the plasma membrane of the cancer cells (Fig. 5). Several sections showed labeling of the majority of cancer cells, whereas in others, only some areas of the tumor were found to be positive for FAK (Fig. 6). As heterogeneous expression of FAK was observed in cancers, FAK expression was evaluated with the criteria described in *Materials and Methods*. Of the 50 invasive ductal adenocarcinomas studied, FAK expression was positive in 24 samples (48%) and negative in 26 samples (52%) (Table 1).

Relationship between FAK Protein Expression and Clinicopathological Features and Survival Rate of the Patients

The relationship between FAK expression and the clinicopathological factors was analyzed (Table 2). There was a statistically significant correlation between FAK expression and tumor size ($P = 0.004$). However, FAK expression did not significantly correlate with other factors such as age, sex, tumor histological grade, lymph node metastasis, distant metastasis, International Union Against Cancer (UICC) stage, portal venous system invasion, nerve invasion, arterial invasion, anterior pancreatic serosal invasion, and retroperitoneal tissue invasion. In terms of the FAK expression status, the survival rate was not statistically different between the two groups (Fig. 7).

DISCUSSION

Focal adhesion kinase has been reported to be strongly expressed by a variety of human tumors including breast, colon, thyroid, head and neck, ovarian, liver, and esophageal cancers, as well as brain, head and neck, thyroid, breast, esophagus, stomach, liver, colon, ovarian, and prostate cancers.[5–9] Several reports on esophageal[9] and hepatocellular carcinomas[15] showed that the survival rate of the patients with FAK-positive cancer was significantly worse than that of the patients with FAK-negative cancer. In addition, it has been reported that FAK expression was stronger in cancer tissues than that in normal tissues.[5,9,15–17] Together with the reports from in vitro experiments,[2–4] FAK has been implicated in the regulation of important cancer cell behaviors such as adhesion, spreading, migration, invasion, metastasis, and apoptosis.

In the present study, we first showed that FAK is upregulated and strongly expressed in all seven pancreatic cancer cell lines at the levels of mRNA, protein, and phosphorylated protein. At the tissue level, we also demonstrated for the first time that FAK was present in 24 of the 50 patients (48%). Therefore, it is speculated that FAK could have some roles in the progression of pancreatic cancer.